THE JOURNAL OF BIOLOGICAL CHEMISTRY VOL. 286, NO. 10, pp. 8555–8564, March 11, 2011

Cellular Up-regulation of Nedd4 Family Interacting Protein 1 (Ndfip1) using Low Levels of Bioactive Cobalt Complexes*[S]

Received for publication, November 19, 2010, and in revised form, December 20, 2010 Published, JBC Papers in Press, December 27, 2010, DOI 10.1074/jbc.M110.203448

Christine Schieber[‡§1], Jason Howitt[§1], Ulrich Putz[§], Jonathan M. White[‡], Clare L. Parish[§], Paul S. Donnelly[‡2], and Seong-Seng Tan[§3]

From the [‡]School of Chemistry, Bio21 Molecular Science and Biotechnology Institute, The University of Melbourne, Parkville 3010, Victoria, Australia and the [§]Florey Neuroscience Institutes and Centre for Neuroscience, The University of Melbourne, Parkville 3010, Victoria, Australia

The delivery of metal ions using cell membrane-permeable metal complexes represents a method for activating cellular pathways. Here, we report the synthesis and characterization of new [Co^{III}(salen)(acac)] complexes capable of up-regulating the ubiquitin ligase adaptor protein Ndfip1. Ndfip1 is a neuroprotective protein that is up-regulated in the brain after injury and functions in combination with Nedd4 ligases to ubiquitinate harmful proteins for removal. We previously showed that Ndfip1 can be increased in human neurons using $CoCl_2$ that is toxic at high concentration. Here we demonstrate a similar effect can be achieved by low concentrations of synthetic Co^{III} complexes that are non-toxic and designed to be activated following cellular entry. Activation is achieved by intracellular reduction of Co^{III} to Co^{II} leading to release of Co^{II} ions for Ndfip1 up-regulation. The cellular benefit of Ndfip1 up-regulation by Co^{III} complexes includes demonstrable protection against cell death in SH-SY5Y cells during stress. *In vivo*, focal delivery of Co^{III} complexes into the adult mouse brain was observed to up-regulate Ndfip1 in neurons. These results demonstrate that a cellular response pathway can be advantageously manipulated by chemical modification of metal complexes, and represents a significant step of harnessing low concentration metal complexes for therapeutic benefit.

Transition metals are essential for many important chemical processes in biological systems. Most of these metal-related processes occur by interactions with nucleic acids and proteins. Within the cell, metal ions can stabilize, destabilize, or modulate DNA and proteins by introducing conformational changes and by creating centers of activity. Although the use of metals as structural elements within the cell is well known, emerging evidence now recasts metals as signaling molecules able to activate critical cellular pathways. For example, metals such as iron, copper, and cobalt can produce reactive oxygen species that lead to the activation of redox-sensitive transcription factors including NF-κB, AP-1, and p53. Metals have also been suggested to affect the upstream regulatory components of the MAP kinase and the PI3K/Akt/mTor pathway (1, 2). Thus the levels and regulation of metals in a cell can have a direct role on cell function and survival.

Metal ions such as Co^{II} and Fe^{II} can stimulate the expression of the neuroprotective protein Nedd4 family interacting protein 1 (Ndfip1)[4] in the brain (3). Ndfip1 is a transmembrane protein that is localized to the Golgi and post-Golgi vesicles such as endosomes (4, 5). Ndfip1 functions as an adaptor protein for the Nedd4 family of ubiquitin ligases that target proteins for both degradation and trafficking (4). The metal-induced up-regulation of Ndfip1 results in the activation of the ubiquitin proteasome pathway. Ndfip1 recognizes and interacts with divalent metal transporter 1 (DMT1), this recruits the E3 ligase Nedd4–2 resulting in degradation of DMT1, preventing iron overload within the cell (3). Other targets for Ndfip1 have also been identified, including the transcription factor JunB that is regulated by Ndfip1 in association with the E3 ligase Itch (6). In the adult brain, Ndfip1 is endogenously present in cortical neurons at low levels, however it is up-regulated in a subset of neurons upon activation by injury or stress (7). Importantly, this up-regulation of Ndfip1 has been shown to be neuroprotective, and neurons with up-regulated Ndfip1 do not undergo apoptosis.

Whereas high levels of exogenous Co^{II} and Fe^{II} are toxic to cells, our previous results show they also stimulate Ndfip1 via still unknown mechanisms. Barring the effects of metal toxicity, this finding introduces an opportunity to harness the capacity of metal ions to up-regulate Ndfip1 for neuroprotective purposes. In the present study, we investigate the utility of non-toxic metal complexes for controlled intracellular delivery of cobalt to stimulate Ndfip1 expression. This was based on the premise that the reactivity of metal ions can be modulated by the formation of coordination complexes, with a complexed

* This study was supported by grants under the Victorian Neurotrauma Initiative of the TAC, and the National Health and Medical Research Council (NH&MRC).

The following crystal structures have been deposited at the Cambridge Crystallographic Data Centre and allocated the deposition numbers CCDC 808949 and 808950.

[S] The on-line version of this article (available at http://www.jbc.org) contains supplemental Figs. S1–S3.

[1] Both authors contributed equally to this work.

[2] To whom correspondence may be addressed: School of Chemistry, Bio21 Molecular Science and Biotechnology Institute, The University of Melbourne, Parkville 3010, Victoria, Australia. Tel.: 61-3-8344-2399; E-mail: pauld@unimelb.edu.au.

[3] To whom correspondence may be addressed: Brain Development and Regeneration Laboratory, Florey Neurosciences Institute, The University of Melbourne, Parkville 3010, Victoria, Australia. Tel.: 61-3-8344-1958; Fax: 61-3-9347-0446; E-mail: stan@florey.edu.au.

[4] The abbreviations used are: Ndfip1, Nedd4 family interacting protein 1; DMT1, divalent metal transporter 1; CHX, cycloheximide; ICP-MS, inductively coupled plasma mass spectrometry.

metal ion having remarkably different reactivity to the "free" metal ion or hydrated cation. The incorporation of metal ions into coordination complexes permits superior control over their reactivity, and minimizes unwanted interactions with other molecules (8). Furthermore, the coordination of metal ions to ligands permits manipulation of their distribution and diffusion properties across cell membranes.

Here we report the design and synthesis of metal complexes capable of delivering cobalt ions into the cell that are bioactive at far lower concentrations than the free metal salts. We demonstrate that this approach is capable of delivering low, but biologically effective levels of cobalt into the cell, resulting in Ndfip1 up-regulation with sustainable biological effects. As proof of concept, we show that cobalt-induced Ndfip1 up-regulation provides protection against cell death from noxious stimuli such as hydrogen peroxide. Our approach centers on the coordination of metal ions with suitable ligands as a powerful means of drug design that can overcome traditional hurdles of metal toxicity without compromising biological outcomes.

EXPERIMENTAL PROCEDURES

General Synthetic Procedures—All reagents and solvents were obtained from standard commercial sources and unless otherwise stated were used as received. ^{1}H and ^{13}C NMR spectra were recorded with a Varian Unity 400 or 500 spectrometer (^{1}H at 500 MHz and ^{13}C at 126 MHz). All NMR spectra were recorded at room temperature. The reported chemical shifts (in parts per million) are referenced relative to residual solvent protons. Mass spectra were recorded using the electrospray technique (positive and negative ion) with a Micromass QUATTRO II triple-quadropole electrospray mass spectrometer. UV-Vis spectra were recorded in PB buffer (20 mM, pH 7.4) with a Shimadzu UV-1650PC UV-Vis spectrophotometer using the UVPC c3.9 software program. HPLC was performed with an HP 1100 ChemStation system using a Supelco Discovery C_{18} column (150 nm × 4.6 mm, 5 μm). The HPLC solvents were 0.1% trifluoroacetic acid in water (solvent A) and 0.1% trifluoroacetic acid in acetonitrile (solvent B). The gradient was 0–100% solvent B in 0–25 min, the flow rate was 1.00 ml/min, and the detection was at 280 nm. Microanalysis for carbon, hydrogen, and nitrogen were carried out by Chemical & Micro-Analytical Services (Belmont, VIC, Australia).

Synthesis—The ligands sal **L^{1}**, MeO-sal **L^{2}**, and EtO-sal **L^{3}** were synthesized according to published literature procedures (9). The corresponding aqua Co^{III} complexes were made following modified procedures by Bailes *et al.* (10).

To a suspension of (*N, N′-Ethylenebis-*(*R*-salicylideneiminato)-cobalt(III)(OH)(H_2O) (with *R* = H, OMe, OEt) (0.7–1 mmol) in ethanol (10 ml) was added an excess of acetylacetone (250 μl), and the resulting solution was stirred at room temperature for 2 h. A dark green precipitate formed, which was collected by filtration, washed with cold ethanol (5 ml), water (5 ml) and diethyl ether (5 ml) and dried *in vacuo* to afford **C1–3** as crystalline green solids.

(*N, N′*-Ethylenebis-(salicylideneiminato)-acetylacetone)cobalt(III) **C1** (170 mg, 72%); δ_H (500 MHz; DMSO-d_6) 8.03 (1 H, s), 7.82 (1 H, s), 7.36 (1 H, dd, *J* 7.8, 1.9), 7.27 (1 H, dd, *J* 7.8, 1.8), 7.22 (1 H, ddd, *J* 8.6, 6.8, 1.8), 7.03–6.97 (2 H, m), 6.71–6.70 (1 H, m), 6.51–6.48 (2 H, m), 5.41 (1 H, s), 4.12–4.01 (2 H, m), 3.78–3.68 (2 H, m), 1.76 (3 H, s), 1.73 (3 H, s); δ_C (125 MHz; DMSO-d_6) 188.8, 186.1, 166.9, 166.6, 166.2, 166.1, 134.6, 133.8, 132.9, 131.8, 124.9, 123.2, 122.1, 118.6, 114.4, 112.7, 98.4, 61.1, 59.1, 26.0, 25.5 (11).

(*N, N′*-Ethylenebis-(2-methoxy-salicylideneiminato)-acetylacetone)cobalt(III) **C2** (190 mg, 82%); δ_H (500 MHz; DMSO-d_6) 8.05 (1 H, s), 7.77 (1 H, s), 7.01 (1 H, dd, *J* 8.0, 1.6), 6.90 (1 H, dd, *J* 8.0, 1.6), 6.81 (1 H, dd, *J* 7.6, 1.6), 6.61 (1 H, dd, *J* 7.6, 1.6), 6.44–6.39 (2 H, m), 5.43 (1 H, s), 4.04–4.02 (2 H, m), 3.75–3.65 (2 H, m), 3.70 (1 H, s), 3.56 (3 H, s), 1.74 (3 H, s), 1.73 (3 H, s); δ_C (125 MHz; DMSO-d_6) 189.1, 186.0, 166.9, 166.5, 157.8, 157.6, 154.7, 152.8, 126.4, 125.7, 123.9, 118.6, 116.1, 115.1, 113.7, 111.8, 98.6, 61.1, 59.3, 56.1, 55.7, 26.0, 25.4; HRMS (ESI^{+}) *m/z* $(M+Na)^{+}$ 507.0942 (507.09201 calculated for $C_{23}H_{25}CoN_2O_6Na$); elemental analysis found: C: 56.43%, H: 5.85%, N: 5.82%; calculated for $C_{23}H_{25}CoN_2O_6$: C: 57.03%, H: 5.20%, N: 5.78%.

(*N, N′*-Ethylenebis-(2-ethoxy-salicylideneiminato)-acetylacetone)cobalt(III) **C3** (200 mg, 89%); δ_H (500 MHz; DMSO-d_6) 8.05 (1 H, s), 7.79 (1 H, s), 7.02 (1 H, dd, *J* 8.0, 1.6), 6.95 (1 H, dd, *J* 8.0, 1.6), 6.81 (1 H, dd, *J* 7.5, 1.6), 6.62 (1 H, dd, *J* 7.5, 1.6), 6.41–6.35 (2 H, m), 5.43 (1 H, s), 4.11–3.94 (6 H, m), 3.77–3.75 (2 H, m), 1.75 (3 H, s), 1.73 (3 H, s), 1.22 (3 H, t, *J* 7.0), 1.03 (3 H, t, *J* 7.0); δ_C (125 MHz; DMSO-d_6) 189.0, 186.0, 166.9, 166.7, 159.2, 158.7, 153.2, 151.8, 127.2, 126.5, 125.2, 121.5, 119.3, 118.7, 114.0, 111.8, 98.5, 64.7, 64.5, 60.8, 59.3, 26.0, 25.5, 15.1, 14.9; HRMS (ESI^{+}) *m/z* $(M+Na)^{+}$ 535.12247 (535.1255 calculated for $C_{25}H_{29}CoN_2O_6Na$); elemental analysis found: C: 57.94%, H: 6.34%, N: 5.55%; calculated for $C_{25}H_{29}CoN_2O_6$: C: 58.59%, H: 5.71%, N: 5.47%. Crystals suitable for x-ray analysis were obtained for **C2** and **C3** after allowing a solution of the complex in DMSO to stand in air.

Electrochemistry—Cyclic voltammograms were recorded with an AUTO-LAB PGSTAT100 using the GPES V4.9 software program and employing a glassy carbon working electrode, a platinum counter electrode and a Ag/Ag^{+} reference electrode. The measurements were carried out in DMF. The solutions contained 1 mM analyte in a 0.1 M tetrabutylammonium tetrafluoroborate. The DMF was dried over 3 Å molecular sieves under an atmosphere of N_2 before use. Each solution was purged with N_2 prior to analysis and measured at ambient temperature under a N_2 atmosphere. Each sample was referenced to an internal reference of ferrocene, which was taken as having an $E^{0'}$ = 0.54 V *versus* SCE.

Crystallography—Intensity data were collected with an Oxford Diffraction Sapphire CCD diffractometer using Cu-Kα radiation (graphite crystal monochromator λ = 1.54184 Å). The temperature during data collection was maintained at 130.0(1) using an Oxford Cryostream low temperature device. Crystal data for **C2** $C_{25}H_{31}N_2O_7SCo$, *M* = 562.51, *T* = 130.0(2) K, λ = 1.5418, Monoclinic, space group $P2_1/n$, *a* = 9.7813(2), *b* = 21.0806(4) *c* = 13.0041(3) Å, β = 102.962(2)°, *V* 2613.06(9) Å^3, Z = 4, D_c = 1.430 Mg M^{-3} μ(Cu-Kα) 6.293 mm^{-1}, F(000) = 1176, crystal size 0.27 × 0.07 × 0.05 mm. 18496 reflections measured, 5151 independent reflections (R_{int} = 0.0452) the final R was 0.0431 [$I > 2\sigma(I)$] and *w*R(F^2) was 0.1058 (all data).

Crystal data for **C3** $C_{25}H_{29}N_2O_6Co$, $M = 512.43$, $T = 130.0(2)$ K, $\lambda = 1.5418$, Monoclinic, space group C2/c, $a = 30.3043(6)$, $b = 10.2537(2)$ $c = 15.5706(3)$ *Å*, $\beta = 103.624(2)°$, V 4702.13(16) Å^3, Z = 8, $D_c = 1.448$ Mg m^{-3} μ(Cu-Kα) 6.097 mm^{-1}, F(000) = 2144, crystal size 0.54 × 0.12 × 0.04 mm. 10860 reflections measured, 4215 independent reflections ($R_{int} = 0.0472$) the final R was 0.0412 [$I > 2\sigma(I)$] and $wR(F^2)$ was 0.1065 (all data).

The following crystal structures have been deposited at the Cambridge Crystallographic Data Centre and allocated the deposition numbers CCDC 808949 and 808950.

MATERIALS AND METHODS

Cell Culture and Co^{III} Complex Addition—SH-SY5Y cells were cultured in RPMI media supplemented with 15% FCS, 2 mM L-glutamate, and 50 g/ml PenStrep. Cultures were maintained at 37 °C in a 5% CO_2 atmosphere. Exposure of cells to Co^{III} complexes: prior to treating with cobalt complexes, cells were seeded into 6-well plates at 4×10^4 cells and incubated for 2 days. The compounds (10 mM stock) were prepared in DMSO and added to cells at 0.1–100 μM. Controls used vehicle of DMSO.

Metal Toxicity Quantification by Flow Cytometry—Toxicity of cobalt complexes was assessed quantitatively by flow cytometry using propidium iodide staining. Briefly, 4×10^5 cells were grown in 6-well plates and incubated for 18 h after addition of cobalt complexes at concentrations ranging from 10 mM-0.1 μM. All cells (adherent and suspension) were harvested and stained with 10 μg/ml propidium iodide and incubated for 15 min before analysis by flow cytometry (FACSCalibur, Becton Dickinson).

Inductively Coupled Plasma Mass Spectrometry—Cells were incubated with cobalt complexes for 1 h in serum-free RPMI media. The cells were scraped into phosphate buffer, an aliquot was taken for protein determination (Protein Microassay; Thermo Scientific), and the remaining cells collected by centrifugation at 1500 rpm for 3 min. Pellets were washed three times in PB buffer. The metal levels were determined in cell pellets by ICP-MS as described previously (12) and converted to fold increase in metal compared with untreated controls.

Co^{II} Release, Fluorescence Quenching Assay—Cells were loaded with 0.25 μM calcein-AM (1 mM stock solution in DMSO) for 30 min at 37 °C in RMPI media. Cells were then washed and resuspended in MES buffer (20 mM MES, 150 mM NaCl, pH 6.7) and 2×10^5cells were transferred to a 96-well flat-bottom transparent plate in triplicate, and fluorescence was recorded using a fluorescence spectrometer microplate reader (excitation 488 nm, emission 518 nm). When fluorescence stabilized, cobalt complexes (10 μM) and vehicle were added to the cell suspension and fluorescence was continuously monitored for 500 s.

Western Blot Assays—Assays to determine Ndfip1 overexpression in response to cobalt complexes were conducted by treating cells with complexes **C1**-**3** at varying concentrations for 2–18 h before analysis by Western blot. Prior to treatment, cells were seeded into 10-cm dishes. The compounds were prepared in DMSO at a stock concentration of 10 mM and control cells were treated with DMSO vehicle at 0.1% (v/v). Cells were harvested at indicated time points, washed with ice-cold PBS and lysed in RIPA buffer (50 mM Tris, pH 8, 100 mM NaCl, 5 mM EDTA, 1% Triton X-100, 0.2% SDS, Protein Inhibitor mixture (Roche)) for 20 min on ice. Cell debris was removed by centrifugation (13,000 rpm, 15 min, 4 °C). Cell lysates were subject to SDS-PAGE before transfer to nitrocellulose membranes. Membranes were incubated with rabbit polyclonal Ndfip1 antibody (3), HSP70 and HIF1-α antibody, followed by the appropriate HRP secondary antibody (Upstate). Blots were detected using Amersham Biosciences ECL reagent (GE Healthcare). All blots are representative of at least three different experiments.

Hydrogen Peroxide Toxicity Assay—SH-SY5Y cells and SH-SY5Y inducible cell line (4×10^5) were grown in 6-well plates and incubated for 18 h with or without complex **C3** at 10 μM before the addition of H_2O_2 at concentrations ranging from 5–25 μM. After 1 h of incubation at 37 °C cells were collected (both adherent and suspension) by trypsinization, centrifuged, and labeled with 10 μg/ml propidium iodide for 15 min at room temperature. Stained cells were quantitatively analyzed by flow cytometry (FACSCalibur, Becton Dickinson).

Compound Injections and Immunohistochemistry—Using a fine glass pipette, coupled to a hamilton syringe, the cortex of adult mouse brains were stereotaxically injected with 3 μl of either 10 μM or 50 μM of complex **C3**, 500 μM $CoCl_2$ or DMSO as a vehicle control. Stereotaxic injection co-ordinates in relation to bregma were, anterior +1.0 mm, lateral −1.5 mm, ventral from the dura −1.25 mm. Six hours after injections brains were collected and frozen in OCT before sectioning at 14 μm. Sections were fixed in 4% paraformaldehyde for 20 min and blocked in 10% normal horse serum in 0.1 M phosphate buffer with 0.2% Triton X-100, and then incubated overnight with rat monoclonal Ndfip1 (1:500) primary antibody. Antibody was detected with Alexa Fluor 594-conjugated goat anti-rat IgG (1:500; Invitrogen). TUNEL was used as a marker of cell death and to determine injection sites. Brain sections were imaged using an Olympus BX51 microscope. Ndfip1 positive neurons were measured for intensity using ImageJ (13). Neurons close to the injection site (<50 μm) were not counted due to injury induced by the needle track.

RESULTS

Chemical Synthesis and Characterization—The complex design is crucial for the proposed delivery of Co^{II}. We chose to employ one tetradentate dianionic ligand and one monoanionic bidentate ligand for the preparation of stable, neutral, lipophilic six coordinate Co^{III} complexes (Fig. 1*A*). These low molecular weight complexes (≤ 500 Da), were designed to have ideal characteristics for membrane and blood-brain-barrier permeability.

Tetradentate Schiff-base ligands derived from salicylaldehyde and aliphatic amines are well known (14). Cobalt complexes of tetradentate Schiff-base ligands have been investigated as mimics of vitamin B_{12} coenzymes and certain Co^{III} Schiff-base complexes are known to have antiviral, antibacterial, and antitumor properties (15, 16). The Schiff-base ligands coordinate to Co^{II} or Co^{III} ions through two amine nitrogen atoms and two phenolic oxygen atoms. This family of proligands can be readily modified with a variety of functional groups on the aromatic ring as well as the amine backbone to

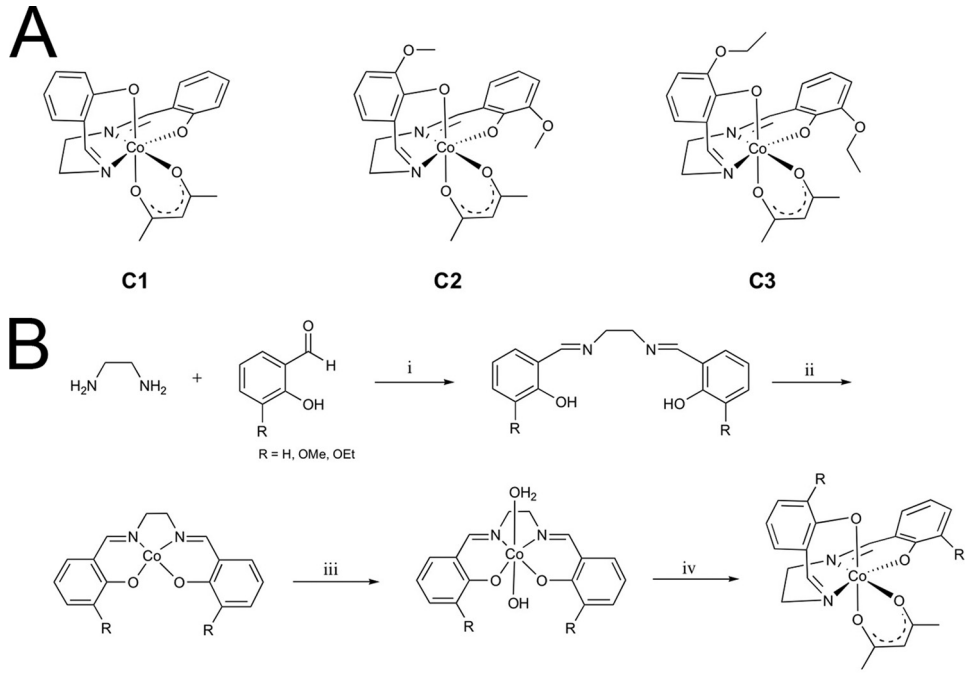

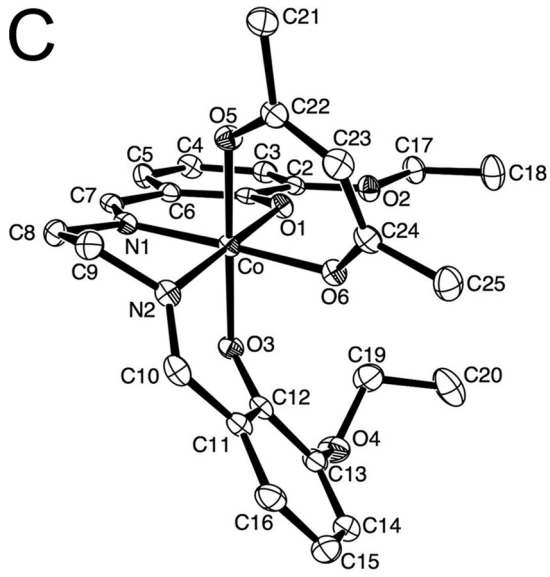

Selected Bond Lengths (Å) and angles (deg)

Co1—N1	1.892(2)
Co1—N2	1.900(2)
O1—Co1	1.8926(17)
O3—Co1	1.8942(18)
O6—Co1	1.9018(17)
O5—Co1	1.9180(18)
N1—Co1—O1	95.03(8)
O1—Co1—N2	176.19(9)
N1—Co1—N2	82.58(9)
N2—Co1—O5	92.50(9)
O3—Co1—O5	179.37(8)

FIGURE 1. **Molecular design of cobalt-complexes.** *A*, structures of cobalt Schiff-base complexes **C1–3**. *B*, synthetic scheme for the synthesis of cobalt complexes **C1–3.** *C*, an ORTEP representation of the molecular structure of **C3** with thermal ellipsoids at 40% probability level. Solvent and hydrogen atoms are omitted for clarity.

alter lipophilicity, cell permeability, and ultimately biodistribution. The final two donor sites of octahedral Co^{III} were supplied by the bidentate ligand anionic acetylacetonate.

The synthesis of **C1**-**3** was carried out as shown in Fig. 1*B*. Ligands were synthesized according to published literature procedures followed by complexation to $Co(OAc)_2$ (9). Oxidation in air in MeOH:H_2O (9:1) followed by the addition of acetylacetone gave the desired neutral complexes (10). All three complexes are diamagnetic as predicted for a low spin d^6 Co^{III} system and were characterized by ^1H and ^{13}C NMR spectroscopy as well as electrospray mass spectrometry and microanalysis. Crystals suitable for single crystal x-ray structure determination of complexes **C2** and **C3** were grown from a saturated solution of the complex in dimethyl sulfoxide. X-ray analysis of compound **C3** shows a neutral cobalt complex with a six-coordinate Co^{III} ion in a distorted octahedral environment (Fig. 1*C*, Table 1, supplemental Fig. S1, **C2** structure). The salen ligand is doubly deprotonated and adopts a twisted arrangement, where the β-diketone occupies two cis-positions of the distorted octahedron around the cobalt atom and the polyhedron being completed by the quadridentate ligand.

Complexes C1–3 Are Stable, Nontoxic, and Allow Cobalt Entry—The cobalt complexes were designed to be kinetically inert to substitution while the cobalt remained in the +3 oxi-

dation state. This should lead to a stable neutral complex capable of diffusing into cells. The electronic absorption spectra of the complexes and uncomplexed ligands gave important information regarding their stability. The electronic absorption spectrum of the ligands $\mathbf{L^1}$-$\mathbf{L^3}$ in DMSO consist of two intense bands centered at about 260 and 320 nm, assigned to the $\pi \rightarrow \pi^*$ transitions of the phenol ring and the azomethine group respectively. The Co^{III} complexes of these ligands (**C1**-**3**) exhibit absorption bands that are red shifted by about 80 nm and appear around 400 nm. These $\pi \rightarrow \pi^*$ azomethine transition bands, show a shoulder at 420 nm, which is attributed to metal-ligand charge transfer transitions ($d \rightarrow \pi^*$). Electronic spectra recorded in 20 mM phosphate buffer (pH 7.4) are slighty shifted with the $\pi \rightarrow \pi^*$ azomethine transition bands located at around 390 nm in the Co^{III} complexes. To show that complexes **C1**-**3** are stable, samples at 10 μM concentration in phosphate buffer were incubated at 37 °C for 24 h. Electronic absorption spectra recorded at 0, 1, and 24 h time points were unchanged suggesting that the complexes remained intact (Fig. 2*A*). It is interesting to note however, that the electronic spectra of the uncomplexed ligands $\mathbf{L^1}$-$\mathbf{L^3}$ in PB buffer showed appreciable changes in a short time at room temperature (Fig. 2*B*). The existence of two well defined isosbestic points indicates that the ligands are susceptible to hydrolysis in aqueous buffer (similar profile for $\mathbf{L^3}$ at 30 min to 3-ethoxysalicylaldehyde) and consequently are unlikely to be stable for appreciable amounts of time once released in the cell.

To determine whether cobalt complexes **C1**-**3** were cell membrane permeable we incubated SH-SY5Y cells with each compound (50 μM, 1 h) and measured intracellular cobalt levels by inductively coupled plasma mass spectrometry (ICP-MS). As expected untreated cells had extremely low levels of cobalt (0.18 ng cobalt/mg protein) (Fig. 2*C*). Signif-

TABLE 1
Crystallographic data for cobalt complexes C2 and C3

	C2	C3
	$[Co(L^2)(acac)].DMSO$	$[Co(L^3)(acac)]$
Chemical Formula	$C_{25}H_{31}CoN_2O_7S$	$C_{25}H_{31}CoN_2O_6$
M	562.51	512.43
Crystal System	Monoclinic	Monoclinic
Temperature/K	130(2)	130(2)
Space Group	P 2_1/n	C 2/c
a/Å	9.7813(2)	30.3043(6)
B/Å	21.0806(4)	10.2537(2)
c/Å	13.0041(3)	15.5706(3)
α/°	90	90
β/°	102.962(2)	103.624(2)
γ/°	90	90
V/Å3	2613.06(9)	4702.13(16)
Z	4	8
Ind Refl.	5151	4251
R(int)	0.0452	0.0472
R (I > 2s(I))	0.0412	0.0412
wR (all data)	0.1065	0.1065

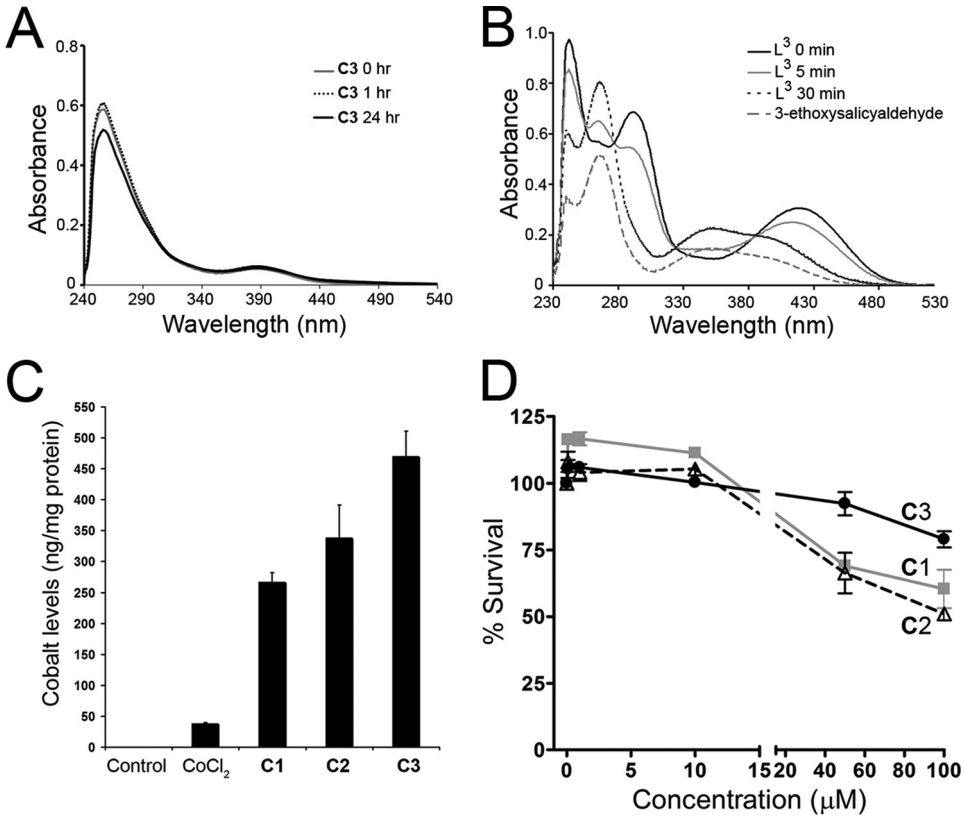

FIGURE 2. **Cobalt complex stability, uptake, and cell viability.** *A*, electronic absorption spectra of complex **C3** in phosphate buffer. The spectra of complex **C3** remains unchanged after incubation at 37 °C for 24 h, demonstrating the stability of the cobalt complex. *B*, electronic absorption spectra of uncomplexed ligand $\mathbf{L^3}$. The spectra of the ligand $\mathbf{L^3}$ shows appreciable changes over a short time at room temperature, indicating that the ligand is susceptible to hydrolysis in aqueous buffer. *C*, cobalt levels in treated SH-SY5Y cells. SH-SY5Y cells were treated with cobalt complexes **C1–3** or $CoCl_2$ (all 50 μM) for 1 h. The metal levels were measured in washed cell pellets by ICP-MS and calculated as ng/mg protein. All cobalt complexes induced significant increases in cellular cobalt levels compared with an untreated control. *D*, cell viability assay. SH-SY5Y cells were treated with complexes **C1–3** for 18 h at concentrations ranging from 0.1–100 μM. Toxicity of cobalt complexes was assessed quantitatively using propidium iodide staining and flow cytometry.

TABLE 2
Cathodic peak potentials E_{pc} of the Co(III) complexes in DMF

		E_{pc}(mV) vs. Fc/Fc^+
Co(salen)(acac)	**C1**	−835
Co(MeO-salen)(acac)	**C2**	−814
Co(Eto-salen)(acac)	**C3**	−864

icant increases of cobalt levels were observed for all three cobalt complexes when compared with $CoCl_2$-treated cells (Fig. 2*C*). The highest levels were induced by treatment with the more lipophilic complex **C3** where a 12-fold increase in intracellular cobalt levels was detected compared with $CoCl_2$. This corresponds to cellular cobalt levels of 38 and 470 ng of cobalt/mg protein for $CoCl_2$ and cobalt complex **C3** respectively. Both complex **C1** and **C2** showed a 6–8-fold increase in cobalt concentration compared with $CoCl_2$. Uptake into cells was highly facilitated by neutral complexes, cationic complexes showed average cobalt leveles of 70 ng of cobalt/mg protein (data not shown).

The effects of complexes **C1-3** on cell viability were determined by a dose-dependent cell survival assay using quantitative flow cytometry and staining for dead cells with propidium iodide. Each complex showed no toxicity up to ~20 μM, after which both complex **C1** and **C2** both started to affect cell survival (Fig. 2*D*). Complex **C3** started to show negative cell survival effects at concentrations above 50 μM. At 100 μM both complex **C1** and **C2** showed ~40% cell death, with complex **C3** being the least toxic with only 20% cell death observed after 24 h incubation. These results show that even though complex **C3** was delivering the highest level of cobalt to the cell it was the least toxic.

Cobalt Complexes Are Reducible by Intracellular Reductants—The electrochemical behavior of complexes **C1-3** was studied by cyclic voltammetry (CV). Cyclic voltammograms were acquired in dimethylformamide solutions of the complexes at a glassy carbon electrode. The cathodic peak potential E_{pc} for each complex was obtained from the CV and referenced to the ferrocene/ferrocenium couple ($E^{0'}$ = 0.54 V *versus* SCE) and these values are summarized in Table 2. Each of the complexes displayed an irreversible reduction attributed to a $Co^{III} \rightarrow Co^{II}$ process at about E_{pc} = −0.80 V. More reversible processes tentatively attributed to $[Co^{II}L] + e^- \rightarrow [CoL]^-$ and to $[Co^{III}L]^+ \rightarrow [Co^{IV}L]^{2+}$ could also be detected, but are less relevant to the present application of complexes **C1-3**. Irreversible redox couples are typical for many Co^{III} complexes, as electrochemical reduction is often followed by a chemical change as a consequence of the lability of Co^{II}. The E_{pc} values for **C1-3** should be accessible for reduction by cellular reductants. The values encountered are within range of other metal complexes that have been shown to be reduced intracellularly (17, 18).

In addition, electronic absorption spectra showed that although complexes **C1-3** were stable for extended periods in aqueous solution, as anticipated, the biologically relevant reductant cysteine reduced complexes **C1-3**. Upon addition of cysteine an immediate change in the electronic absorption spectra was observed, consistent with reduction to Co^{II} and ligand exchange (supplemental Fig. S2).

Co^{II} Is Released from Complexes following Reduction by Intracellular Reductants—Our approach of delivering bioavailable Co^{II} is based on cobalt having a kinetically inert higher oxidation state, Co^{III} and a more kinetically labile lower oxidation state, Co^{II}. Kinetically inert transition metal complexes, such as Co^{III} are known to undergo the water exchange reaction relatively slowly, with half-lives of about 1 day (19). In contrast, the divalent oxidation state is known for its labile metal complexes with ligand exchange occurring rapidly. This means that for redox cycling to occur, back-oxidation would have to be quicker then the rate of ligand release, which is unlikely considering the rate of aquation of cobalt complexes is in the order of 10^6 s^{-1} (20). To determine whether Co^{II} is released following reduction by intracellular reductants we carried out a fluorescence quenching assay (21). The acetomethoxy derivate of calcein (calcein-AM) is non fluorescent and can be transported through the cellular membranes, where intracellular esterases remove the acetomethoxy groups resulting in a strong green fluorescence. It is known, that the fluorescence of calcein is quenched strongly by divalent metal ions such as Co^{II}, Ni^{II}, and Cu^{II} at physiological pH (22). The addition of **C1-3** (10 μM) to SH-SY5Y cells, loaded with calcein dye at 250 nM resulted in a rapid quenching of fluorescence indicating that cobalt was released from each of the complexes (Fig. 3, *A* and *B*). Both complexes **C1** and **C2** showed very similar rates of fluorescence quenching and as observed above (Fig. 2*C*) they also have similar levels of cobalt entry, therefore they appear to be reduced inside the cell at a similar rate. Complex **C3** displayed the most rapid fluorescence quenching indicating that it can be rapidly reduced to release the cobalt ion once inside the cell. This complex however also has the highest level of cobalt delivery to the cell (Fig. 2*C*) so a combination of rapid cell entry and intracellular reduction may be occurring for this complex. A control experiment confirmed that calcein-fluorescene was not quenched by the Co^{III} complexes **C1–3** in a cell-free assay carried out in phosphate buffer (data not shown).

Cobalt Complexes C1–3 Are Potent at Increasing Ndfip1 Expression—Complexes **C1-3** were designed to deliver bioavailable cobalt to cells in order to upregulate the levels of Ndfip1 protein. To determine the affect of complexes **C1–3** on Ndfip1 expression we incubated SH-SY5Y cells with 10 μM of each complex for 4 h. For comparison cells were also incubated with 200 μM of $CoCl_2$ that we have previously shown to stimulate Ndfip1 expression. All three complexes were able to upregulate Ndfip1 compared with control cells with complex **C2** and **C3** able to stimulate Ndfip1 up-regulation above the levels of $CoCl_2$ (Fig. 4, *A* and *B*). Similar results were observed when 1 μM of each complex was incubated for 18 h, the free ligand without cobalt was observed to show no increase in Ndfip1 expression (supplemental Fig. S3). Addition of cycloheximide (CHX) to cultures inhibited the up-regulation of Ndfip1 protein levels indicating that the increase in Ndfip1 was a result of new protein expression and not due to enhanced stability of Ndfip1 protein (Fig. 4, *C* and *D*).

Addition of cobalt to cells in normoxic conditions results in the stabilization of the α-subunit of hypoxia inducible factor (HIF-1) by blocking its ubiquitination and proteasomal degra-

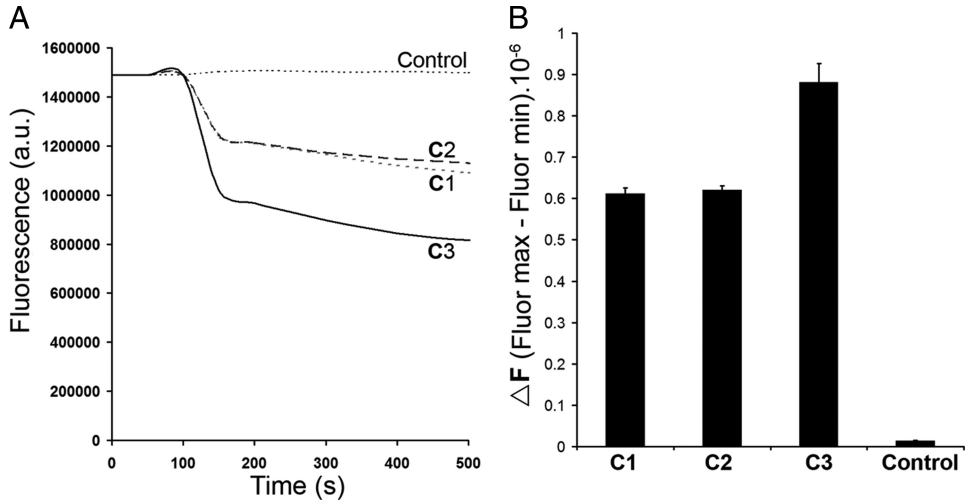

FIGURE 3. **Co^{II} is released from complexes C1–3 following reduction by intracellular reductants.** *A*, calcein fluorescence quenching assay. SH-SY5Y cells were loaded with the metal-sensitive fluorescent dye calcein (introduced as 0.25 μM calcein-AM) for 30 min at 37 °C. Cells were washed and resuspended in MES buffer. A total of 10 μM cobalt complex **C1–3** was added to the cells and the rate of fluorescence quenching measured at 560 nm. *B*, analysis of the rate of calcein fluorescence quenching from *B*.

dation (23). We investigated the affect of complex **C1**-**3** and $CoCl_2$ on HIF1-α levels in SH-SY5Y cells after 6 h of incubation. As expected $CoCl_2$ was observed to increase the levels of HIF1-α (either 200 or 400 μM), surprisingly all three complexes failed to show an increase the levels of HIF1-α (Fig. 4*E*) despite showing an increase in the levels of intracellular cobalt (Fig. 2*C*). To further study the cellular response occurring due to cobalt complexes we investigated the activation of HSP-70 after incubation with either $CoCl_2$ or complex **C3** for 18 h. HSP-70 is known to be activated due to heat shock as well as a general stress response and in SH-SY5Y cells we observed robust up-regulation of HSP-70 levels after both heat shock and $CoCl_2$ (200 μM) treatment (Fig. 4*F*). Complex **C3** was also observed to activate HSP70 at 100 μM although at a lower level compared with heat shock or $CoCl_2$ treatment, lower concentrations of complex **C3** did not result in HSP70 levels above control levels (Fig. 4*F*).

Cobalt Complexes Protect SH-SY5Y Cells from H_2O_2-induced Toxicity—Using an inducible SH-SY5Y cell line, where Ndfip1 expression is up-regulated following induction with 4-hydroxy tamoxifen, we showed protection from H_2O_2 induced toxicity (Fig. 4*G*). To investigate the biological effect of Ndfip1 up-regulation as a response to cobalt complex exposure we incubated SH-SY5Y cells with complex **C3** for 18 h at a concentration of 10 μM before the addition of 5–25 μM H_2O_2 to the culture media for 1 h. Cell survival was assayed by flow cytometry and staining with propidium iodide for cell death. Cells treated with complex **C3** showed a significant decrease in cell death compared with control cells (Fig. 4*H*). The level of protection observed after complex **C3** treatment was similar to that observed for the Ndfip1 induced cells. Overall these findings indicate that the treatment of complex **C3** results in the involvement of Ndfip1 in mediating cell signaling pathways that ultimately lead to cell survival.

In Vivo Up-regulation of Ndfip1 in Neurons Treated with Complex C3—To determine if complex **C3** could up-regulate Ndfip1 *in vivo* we used stereotaxic injections of control vehicle (2% DMSO), or vehicle containing 10 μM or 50 μM complex **C3** or 500 μM $CoCl_2$ into the cortex of adult mice. Levels of Ndfip1 expression were determined through immunohistochemistry and quantitative analysis of fluorescence levels using ImageJ. We observed that 500 μM $CoCl_2$ was able to up-regulate Ndfip1 levels *in vivo* (Fig. 5, *A–C*) supporting our previous findings of $CoCl_2$ up-regulation of Ndfip1 in human primary neuron cultures (3). Injection of complex **C3** at both 10 and 50 μM was able to significantly up-regulate Ndfip1 at levels comparable to 500 μM $CoCl_2$, whereas vehicle was found to have no effect on Ndfip1 levels (Fig. 5, *A–C*).

DISCUSSION

The regulation of protein expression in the cell is essential not only for normal homeostasis but also critical at times of stress when cells are challenged by adverse environments. Here we report a novel application of cobalt metal complexes to up-regulate protein expression of Ndfip1, a known neuroprotectant (3, 7). The designed compounds were effective at micromolar levels in their ability to up-regulate Ndfip1 expression. We have previously demonstrated that Ndfip1 can be up-regulated in response to metal-induced stress from iron and cobalt exposure, and the up-regulation is effective in protecting neurons from metal toxicity (3). How this is achieved remains unclear, but one possibility is ubiquitin-mediated degradation of harmful proteins following binding to Ndfip1 (24). For example, a proposed mechanism for cell protection is binding of up-regulated Ndfip1 to the metal transport protein DMT1, leading to its ubiquitination and degradation in the proteasome, thereby limiting further metal entry (3). This suggests that manipulating intracellular levels of metal ions within subtoxic thresholds can control Ndfip1 expression, providing leverage to intracellular events lying downstream of Ndfip1 activity. However, a key challenge in activating Ndfip1 levels is the high concentration (and toxic levels) of metal ions required for up-regulation. Therefore, a novel aspect of the present work is the exploitation of relatively benign metal complexes for cellular entry leading to metal ion release under the reducing conditions present within the cell. This approach is based on cobalt

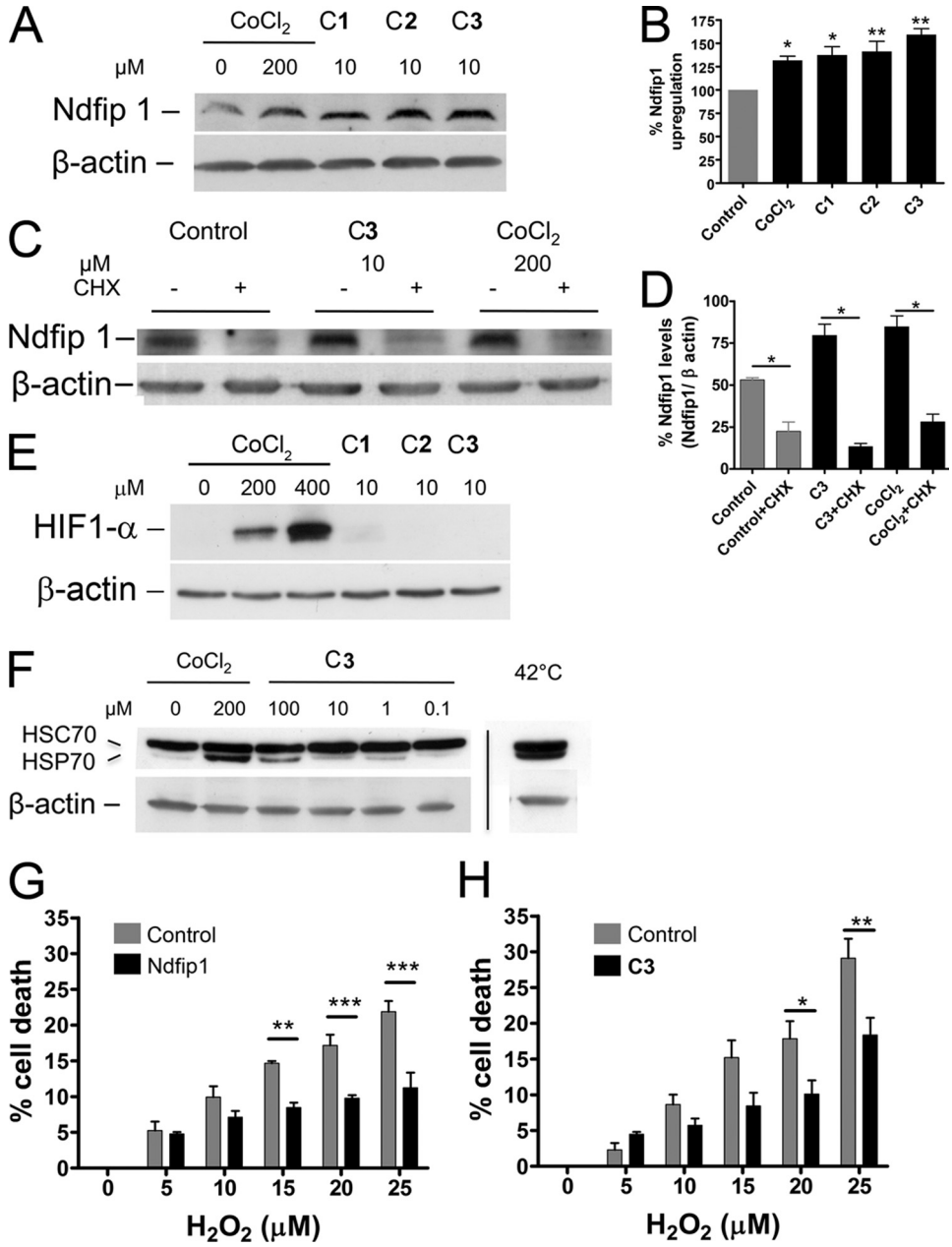

FIGURE 4. **Ndfip1 is up-regulated by complexes C1–3.** *A*, SH-SY5Y cell lysates after exposure to cobalt chloride ($CoCl_2$) and complexes **C1**-**3** for 4 h results in increased Ndfip1 expression. Representative blots are shown from three independent experiments. *B*, quantification of Western blots in A (Dunnett's multiple comparison test, $p < 0.05$, *; $p < 0.01$, **). *C*, increase in Ndfip1 protein in metal-treated cells is due to increased protein expression. SH-SY5Y cells treated with **C3** or $CoCl_2$ up-regulate Ndfip1. Treatment with CHX for 6 h prevents the increased expression of Ndfip1 in response to **C3** or $CoCl_2$. *D*, quantification of Western blots in *C* (*t* test, $p < 0.05$, *). *E*, levels of HIF1-α protein after exposure to metals. Cobalt complexes **C1–3** do not show an increase in the levels of the hypoxia inducible protein HIF1-α after incubation for 6 h. *F*, activation of HSP70 after exposure to metals. HSP70 was robustly up-regulated after heat shock (42 °C) and after exposure to $CoCl_2$. Complex **C3** activates HSP70 at 100 μM, although at lower level compared with heat shock or $CoCl_2$ treatment. Lower concentrations of complex **C3** did not activate HSP70 above control levels. *G*, hydrogen peroxide insult of SH-SY5Y cells. Flow cytometry analysis of SH-SY5Y cells induced by 4-hydroxy tamoxifen to overexpress Ndfip1 before exposure to H_2O_2 stress for 1 h. Cells induced to express Ndfip1 showed significantly less cell death compared with uninduced control. *H*, flow cytometry analysis of SH-SY5Y cells treated with 10 μM complex **C3** for 18 h prior to insult with hydrogen peroxide. Cells treated with complex **C3** show a significant reduction in cell death compared with untreated controls. Two-way ANOVA tests (Bonferroni post-tests) indicate significant protection by Ndfip1 at higher concentrations of hydrogen peroxide (*E*) and (*F*) ($p < 0.05$, *; $p < 0.01$, **; and $p < 0.001$,***; S.E.). Each flow cytometric analysis represents three independent experiments.

having an inert higher oxidation state Co^{III} and a less stable lower oxidation state, Co^{II}. Complexes have been designed to be neutral, membrane permeable and yet kinetically inert to substitution in their Co^{III} oxidation state. Once inside the cell, complexes are reduced to the corresponding Co^{II} complexes that are substitutionally labile and as a consequence release bioactive Co^{II}.

The success of this Trojan horse approach hinges not only on effective delivery of biologically inert Co^{III} metal complexes into the cell, but also demonstration that once inside the cell, the complexes are converted into biologically active Co^{II}. Evidence in support of this was obtained using cyclic voltammetry and electronic absorption measurements showing that the Co^{III} metal complexes are susceptible to reduction by intracellular

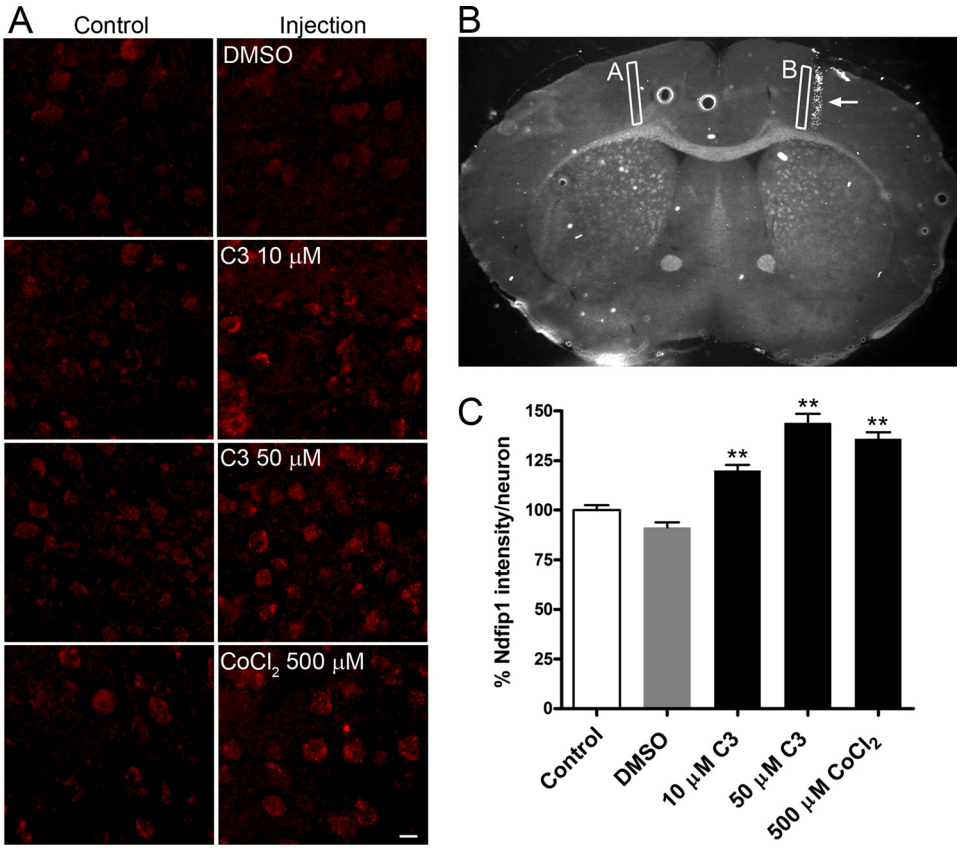

FIGURE 5. ***In vivo* up-regulation of Ndfip1 by complex C3 in the mouse cortex.** *A*, stereotaxic injections of complex **C3** (10 μM and 50 μM), $CoCl_2$ and DMSO vehicle were performed and brains removed after 6 h. Immunohistochemical staining for Ndfip1 of the injected brains, noninjected hemispheres were used as the controls (scale bar, 10 μm). *B*, coronal brain slice illustrating the injection site (*arrow*) as highlighted by TUNEL staining. Regions A and B indicate the area were Ndfip1 positive neurons have been counted (~600 μm^2). *C*, Ndfip1 staining intensity counts for neurons from regions A and B for complex **C3**, $CoCl_2$ and DMSO vehicle. Injections were performed on 3 animals per sample, and two sections per animal surrounding the injection site were counted. Data represent ± S.E., one-way ANOVA test (Dunnett's post test) with significant up-regulation of Ndfip1 following **C3** and $CoCl_2$ administration (**, $p < 0.01$).

reductants to the labile Co^{II} oxidation state. Additional evidence of metal release was provided by a fluorescence quenching assay to directly monitor the release of Co^{II} (21). Of the three complexes under study, complex **C3** showed the highest rate of calcein fluorescene quenching, suggesting that **C3** has a greater rate of Co^{II} release. The greater potency of complex **C3** is most likely related to its design involving ethyl substituents, rendering it more membrane permeable, or alternatively, more susceptible to reduction once inside the cell. As only Co^{II} is capable of quenching the calcein fluorescence the data confirms that dissociation of the metal from the ligands inside the cell allows for the release of bioavailable Co^{II}.

Ndfip1 up-regulation by complex **C3** is biologically meaningful, as demonstrated by its ability to protect cultured cells from death following exposure to hydrogen peroxide *in vitro*. The degree of protection is comparable to the effect observed within cells engineered to overexpress Ndfip1 by genetic means (3). We found that following stereotaxic injection of complex **C3** into the cortex, Ndfip1 was up-regulated in neurons situated over an area ~600 μm^2 adjacent the injection site, suggesting its capacity to function *in vivo*. This effect was also elicited by high concentrations of the $CoCl_2$ salt, suggesting that complex **C3** is equally effective in perfusing the cell matrix as the free salt. Currently it is unclear whether complex **C3** has the capability to remain stable and travel through intercellular spaces to activate neurons further from the injection site.

A further advance in using the present approach is the low (micromolar) concentrations of cobalt complexes required for generating a biological effect when compared with the use of simple metal salts such as $CoCl_2$. This is related to the high efficiency of cobalt complex uptake followed by complex reduction inside the cell releasing bioavailable Co^{II}. We found this to be the case for all three complexes tested, which despite subtle differences in their design, are capable of Ndfip1 up-regulation at 1 μM concentration, compared with 200 μM for $CoCl_2$. Their effectiveness at micromolar concentrations presents significant therapeutic potential without the side effects of metal toxicity. Our findings also have strong implications for the current use of high (200–500 μM) levels of $CoCl_2$ for experimental modeling of hypoxia (25–27). In those studies it is frequently assumed that cobalt ions simulate hypoxic stress by direct activation of the promoter elements of HIF1-α gene or by redox activity of excess Co^{II} causing reactive oxygen species production. By contrast the current study demonstrates that cobalt complexes **C1**-**3** at concentrations of 10 μM, where higher levels of the metal are entering the cell compared with $CoCl_2$ incubation, do not upregulate the stress reporter protein HSP70 or the hypoxia-stimulated protein HIF1-α (28, 29). These results suggest that unlike treatment with $CoCl_2$, the up-regula-

tion of Ndfip1 using cobalt complexes **C1**-**3** is unlikely to be the result of a general cell stress response. It can also been inferred from the results that activation of HIF1-α or indeed HSP70 requires metal entry via a transporter on the cell surface for effective response. Significantly, these findings open up new opportunities for studying how cobalt ions cause cellular hypoxic stress and how cells are able to sense their surrounding environment.

The potential for cobalt coordination complexes as therapeutic agents has previously been investigated by others (30, 31). It is noteworthy that in those complexes, the metal ion plays the role of a carrier and provides an inert framework for transportation of a cytotoxic agent, such as nitrogen mustards, but performs no direct action in the biological system. In the case of nitrogen mustards the formation of a coordination bond between the Co^{III} ion and a nucleophilic amine or oxygen masks the cytotoxicity of the compound and allows for bioreductive activation. In contrast, we synthesized Co^{III} complexes designed to deliver Co^{II} in the cellular environment. The complexes presented here employ one tetradentate dianionic ligand and one monoanionic bidentate ligand resulting in the formation of stable, neutral, lipophilic six coordinate Co^{III} complexes. The tetradentate system are well known ligands derived from the condensation of 1,2-diaminoethane with substituted salicaldehydes to give proligands often given the trivial name salenH_2. Complex **C1** has previously been synthesized with unknown biological activity, but complexes **C2** and **C3** are novel. Complexes **C2** and **C3** bear methyl/ethyl substituents in the 2-position of the phenol ring to influence their lipophilicity and cellular uptake. All three complexes are membrane permeable, shown by measuring intracellular cobalt levels using ICP-mass spectrometry of treated SH-SY5Y cells. However complex **C3** was observed to have properties that allow for a greater amount and rate of cobalt entry.

The present work may be interpreted in the wider context of using metal ions for therapeutic purposes (2, 32). Alterations in metal homeostasis are connected to severe human disorders, including cancer, diabetes and neurodegenerative diseases (33). Changes to transition metal-ion homeostasis have been implicated in a number of neurodegenerative conditions and therapeutic approaches that target transition metal ion metabolism, specifically copper and zinc, have shown promise in the treatment of Alzheimer disease (1, 32). For example, copper-bis(thiosemicarbazone) complexes such as Cu^{II}(gtsm) can cross the blood-brain barrier and increase cellular metal ion bioavailability, leading to inhibition of glycogen synthase kinase 3β (GSK3β), which ultimately results in degradation of Aβ and tau phosphorylation (1). In the present study, direct introduction of cobalt complex **C3** into the adult mouse brain was efficient in increasing neuronal levels of Ndfip1. We propose that targeted delivery of such metals allows for the activation of intracellular pathways and have demonstrated this through the up-regulation of the neuroprotective protein Ndfip1.

Acknowledgments—We thank Anh Doan and Alison Macintyre for excellent technical assistance.

REFERENCES

1. Crouch, P. J., Hung, L. W., Adlard, P. A., Cortes, M., Lal, V., Filiz, G., Perez, K. A., Nurjono, M., Caragounis, A., Du, T., Laughton, K., Volitakis, I., Bush, A. I., Li, Q. X., Masters, C. L., Cappai, R., Cherny, R. A., Donnelly, P. S., White, A. R., and Barnham, K. J. (2009) *Proc. Natl. Acad. Sci. U.S.A.* **106,** 381–386
2. Donnelly, P. S., Caragounis, A., Du, T., Laughton, K. M., Volitakis, I., Cherny, R. A., Sharples, R. A., Hill, A. F., Li, Q. X., Masters, C. L., Barnham, K. J., and White, A. R. (2008) *J. Biol. Chem.* **283,** 4568–4577
3. Howitt, J., Putz, U., Lackovic, J., Doan, A., Dorstyn, L., Cheng, H., Yang, B., Chan-Ling, T., Silke, J., Kumar, S., and Tan, S. S. (2009) *Proc. Natl. Acad. Sci. U.S.A.* **106,** 15489–15494
4. Harvey, K. F., Shearwin-Whyatt, L. M., Fotia, A., Parton, R. G., and Kumar, S. (2002) *J. Biol. Chem.* **277,** 9307–9317
5. Putz, U., Howitt, J., Lackovic, J., Foot, N., Kumar, S., Silke, J., and Tan, S. S. (2008) *J. Biol. Chem.* **283,** 32621–32627
6. Oliver, P. M., Cao, X., Worthen, G. S., Shi, P., Briones, N., MacLeod, M., White, J., Kirby, P., Kappler, J., Marrack, P., and Yang, B. (2006) *Immunity* **25,** 929–940
7. Sang, Q., Kim, M. H., Kumar, S., Bye, N., Morganti-Kossman, M. C., Gunnersen, J., Fuller, S., Howitt, J., Hyde, L., Beissbarth, T., Scott, H. S., Silke, J., and Tan, S. S. (2006) *J. Neurosci.* **26,** 7234–7244
8. Hambley, T. W. (2007) *Dalton Trans.* 4929–4937
9. Zhang, X., Zhou, H., Su, X., Chen, X., Yang, C., Qin, J., and Inokuchi, M. (2007) *J. Alloys Compd.* **432,** 247–252
10. Bailes, R. H., and Calvin, M. (1947) *J. Am. Chem. Soc.* **69,** 1886–1893
11. Cozens, R. J., and Murray, K. S. (1972) *Aust. J. Chem.* **25,** 911–917
12. White, A. R., and Cappai, R. (2003) *J. Neurosci. Res.* **71,** 889–897
13. Abramoff, M. D., Magelhaes, P. J., and Ram, S. J. (2004) *Biophotonics Int.* **11,** 36–42
14. Yamada, S. (1966) *Coord. Chem. Rev.* **1,** 415–437
15. Dreos, R., Nardin, G., Randaccio, L., Siega, P., Tauzher, G., and Vrdoljak, V. (2003) *Inorg. Chim. Acta* **349,** 239–248
16. Bigotto, A., Costa, G., Mestroni, G., Nardin-Stefani, L., Puxeddu, A., Reisenhofer, E., and Tauzher, G. (1970) *Inorg. Chim. Acta, Rev.* **4,** 41–49
17. Yamamoto, N., Danos, S., Bonnitcha, P. D., Failes, T. W., New, E. J., and Hambley, T. W. (2008) *J. Biol. Inorg. Chem.* **13,** 861–871
18. Failes, T. W., Cullinane, C., Diakos, C. I., Yamamoto, N., Lyons, J. G., and Hambley, T. W. (2007) *Chem. Eur. J.* **13,** 2974–2982
19. Teicher, B. A., Abrams, M. J., Rosbe, K. W., and Herman, T. S. (1990) *Cancer Res.* **50,** 6971–6975
20. Fujii, Y. (1970) *Bull. Chem. Soc. Jpn.* **43,** 1722–1728
21. Foot, N. J., Dalton, H. E., Shearwin-Whyatt, L. M., Dorstyn, L., Tan, S. S., Yang, B., and Kumar, S. (2008) *Blood* **112,** 4268–4275
22. Picard, V., Govoni, G., Jabado, N., and Gros, P. (2000) *J. Biol. Chem.* **275,** 35738–35745
23. Epstein, A. C., Gleadle, J. M., McNeill, L. A., Hewitson, K. S., O'Rourke, J., Mole, D. R., Mukherji, M., Metzen, E., Wilson, M. I., Dhanda, A., Tian, Y. M., Masson, N., Hamilton, D. L., Jaakkola, P., Barstead, R., Hodgkin, J., Maxwell, P. H., Pugh, C. W., Schofield, C. J., and Ratcliffe, P. J. (2001) *Cell* **107,** 43–54
24. Mund, T., and Pelham, H. R. B. (2010) *Proc. Natl. Acad. Sci. U.S.A.* **107,** 11429–11434
25. Choi, J. H., Cho, H. K., Choi, Y. H., and Cheong, J. H. (2009) *Biochem. J.* **424,** 285–296
26. Björklund, O., Shang, M., Tonazzini, I., Daré, E., and Fredholm, B. B. (2008) *Eur. J. Pharmacol.* **596,** 6–13
27. Tan, X. L., Huang, X. Y., Gao, W. X., Zai, Y., Huang, Q. Y., Luo, Y. J., and Gao, Y. Q. (2008) *Neurosci. Lett.* **441,** 272–276
28. Mayer, M. P., and Bukau, B. (2005) *Cell. Mol. Life Sci.* **62,** 670–684
29. Aït-Aïssa, S., Porcher, J., Arrigo, A., and Lambré, C. (2000) *Toxicology* **145,** 147–157
30. Hall Matthew, D., Failes Timothy, W., Yamamoto, N., and Hambley Trevor, W. (2007) *Dalton Trans.* 3983–3990
31. Hambley, T. W. (2007) *Science* **318,** 1392–1393
32. White, A. R., Du, T., Laughton, K. M., Volitakis, I., Sharples, R. A., Xilinas, M. E., Hoke, D. E., Holsinger, R. M., Evin, G., Cherny, R. A., Hill, A. F., Barnham, K. J., Li, Q. X., Bush, A. I., and Masters, C. L. (2006) *J. Biol. Chem.* **281,** 17670–17680
33. Bush, A. I. (2000) *Curr. Opin. Chem. Biol.* **4,** 184–191

Supplementary 1

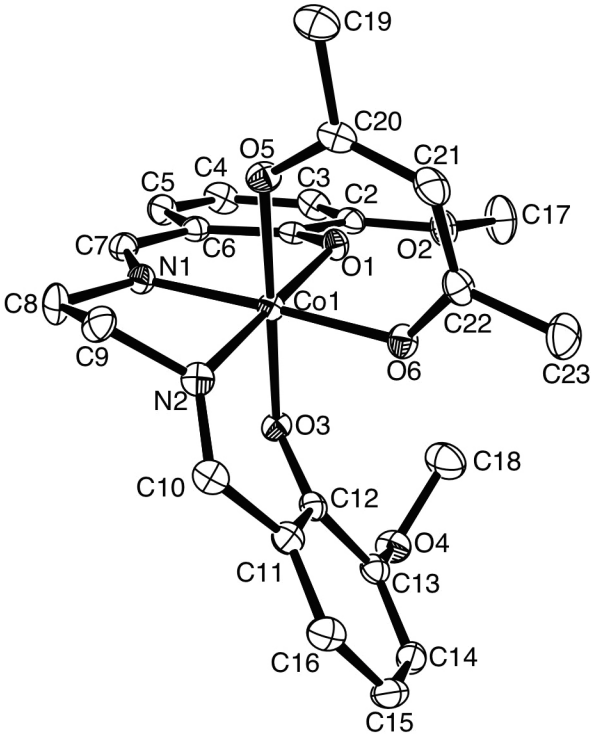

Crystal structure of compound **C2**.

Supplementary 2

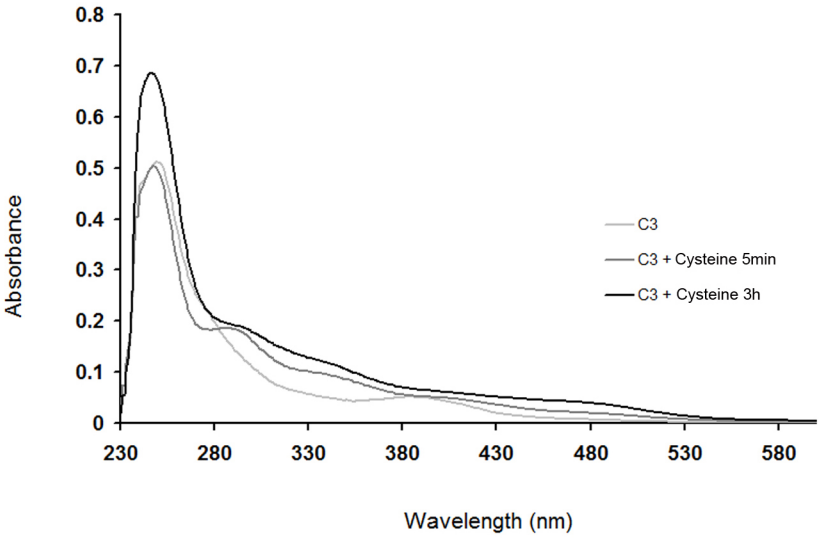

Reduction of **C3** in the presence of cysteine.

Supplementary 3

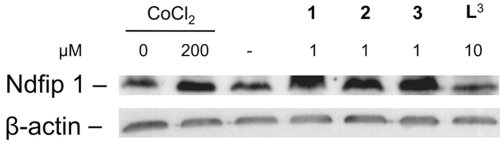

Western blot for Ndfip1 after incubation of SH-SY5Y cells with cobalt compounds and the free ligand for 18h.

Cellular Up-regulation of Nedd4 Family Interacting Protein 1 (Ndfip1) using Low Levels of Bioactive Cobalt Complexes

Christine Schieber, Jason Howitt, Ulrich Putz, Jonathan M. White, Clare L. Parish, Paul S. Donnelly and Seong-Seng Tan

J. Biol. Chem. 2011, 286:8555-8564.
doi: 10.1074/jbc.M110.203448 originally published online December 27, 2010
